catalysts

MDPI

Article

Plant Extract Mediated Eco-Friendly Synthesis of Pd@Graphene Nanocatalyst: An Efficient and Reusable Catalyst for the Suzuki-Miyaura Coupling

Mujeeb Khan [1], Mufsir Kuniyil [1], Mohammed Rafi Shaik [1], Merajuddin Khan [1,*], Syed Farooq Adil [1], Abdulrahman Al-Warthan [1], Hamad Z. Alkhathlan [1], Wolfgang Tremel [2], Muhammad Nawaz Tahir [2] and Mohammed Rafiq H. Siddiqui [1,*]

[1] Department of Chemistry, College of Science, King Saud University, P.O. 2455, Riyadh 11451, Saudi Arabia; kmujeeb@ksu.edu.sa (Muj.K.); mufsir@gmail.com (Muf.K.); rafiskm@gmail.com (M.R.S.); sfadil@ksu.edu.sa (S.F.A.); awarthan@ksu.edu.sa (A.A.-W.); khathlan@ksu.edu.sa (H.Z.A.)

[2] Institute of Inorganic and Analytical Chemistry, Johannes Gutenberg-University of Mainz, Duesbergweg, 55128 Mainz, Germany; tremel@uni-mainz.de (W.T.); tahir@uni-mainz.de (M.N.T.)

* Correspondence: mkhan3@ksu.edu.sa (Me.K.); rafiqs@ksu.edu.sa (M.R.H.S.); Tel.: +966-11-467-5910 (Me.K.); +966-1-467-6082 (M.R.H.S.)

Academic Editor: Ioannis D. Kostas
Received: 27 November 2016; Accepted: 5 January 2017; Published: 9 January 2017

Abstract: Suzuki-Miyaura coupling reaction catalyzed by the palladium (Pd)-based nanomaterials is one of the most versatile methods for the preparation of biaryls. However, use of organic solvents as reaction medium causes a big threat to environment due to the generation of toxic byproducts as waste during the work up of these reactions. Therefore, the use of water as reaction media has attracted tremendous attention due to its environmental, economic, and safety benefits. In this study, we report on the synthesis of green Pd@graphene nanocatalyst based on an in situ functionalization approach which exhibited excellent catalytic activity towards the Suzuki–Miyaura cross-coupling reactions of phenyl halides with phenyl boronic acids under facile conditions in water. The green and environmentally friendly synthesis of Pd@graphene nanocatalyst (PG-HRG-Pd) is carried out by simultaneous reduction of graphene oxide (GRO) and $PdCl_2$ using *Pulicaria glutinosa* extract (PGE) as reducing and stabilizing agent. The phytomolecules present in the plant extract (PE) not only facilitated the reduction of $PdCl_2$, but also helped to stabilize the surface of PG-HRG-Pd nanocatalyst, which significantly enhanced the dispersibility of nanocatalyst in water. The identification of PG-HRG-Pd was established by various spectroscopic and microscopic techniques, including, high-resolution transmission electron microscopy (HRTEM), X-ray diffraction (XRD), ultraviolet–visible spectroscopy (UV-Vis), Fourier transform infrared spectroscopy (FT-IR), and Raman spectroscopy. The as-prepared PG-HRG-Pd nanocatalyst demonstrated excellent catalytic activity towards the Suzuki-Miyaura cross coupling reactions under aqueous, ligand free, and aerobic conditions. Apart from this the reusability of the catalyst was also evaluated and the catalyst yielded excellent results upon reuse for several times with marginal loss of its catalytic performance. Therefore, the method developed for the green synthesis of PG-HRG-Pd nanocatalyst and the eco-friendly protocol used for the Suzuki coupling offers a mild and effective substitute to the existing protocols and may significantly contribute to the endeavors of green chemistry.

Keywords: green synthesis; plant extract; palladium; graphene and Suzuki-Miyaura coupling

1. Introduction

Catalysis plays a very important role in many aspects of life, ranging from academic research to the chemical industry [1]. In the absence of catalysts, manufacturing of several essential commodities

would not be possible at affordable prices—such as medicines, polymers, paints, lubricants, and various types of fine chemicals [2,3]. So far, the field of catalysis has made remarkable advances in the development of several catalytic processes for various important organic transformations including C–H bond activations, chemoselective oxidation and reductions, asymmetric hydrogenations, oxidative aminations, etc. [4,5]. Apart from these catalytic transformations, the cross-coupling reactions for the creation of C–C bonds, such as Heck coupling, Stille, Sonogashira, Kumada, and Suzuki-Miyaura coupling reactions have gained immense interest in several fields [6]. These reactions have been extensively applied for the vast industrial organic transformations, including for the production of agrochemicals, pharmaceuticals, and various other fine chemicals [7].

Among various coupling reactions, the Suzuki–Miyaura coupling has become the most powerful tool for the formation of C–C bonds, which is a transition-metal-catalyzed cross-coupling between an organoboron compound and an organic (pseudo) halide [8]. The Suzuki–Miyaura couplings have gained immense popularity due to their mild reaction conditions, wide range of functional group tolerance, high stability, and easy availability of organoboron reagents [9]. Although, several transitional-metal-based catalysts have been investigated for the Suzuki–Miyaura cross-coupling but palladium-based heterogeneous catalysts have so far gained great success, due to their robust ligand design [10–12]. Particularly, due to the rapid advancement of nanotechnology, Pd nanoparticle (NP)-based heterogeneous nanocatalysts have emerged as excellent substitutes to other organometallic-based conventional materials, which are found to be robust and possessing high surface area and that were used as catalyst support for Suzuki–Miyaura cross-coupling [13,14].

The nano-sized Pd-based catalysts enhances the surface area many folds which results in increasing the contact between substrate and catalyst, and their insolubility in reaction solvents facilitates effortless separation [15]. In order to further enhance the efficiency, cost effectiveness of Pd-based nanocatalysts, different types of support materials are required which facilitate stabilization and homogeneous dispersion of nanocatalyst [16]. So far, silica-based support materials, due to their excellent stability and porosity, have been commonly applied for the Suzuki–Miyaura cross-couplings reactions [17]. Apart from this, many carbon-based support materials have also been applied, as their high specific surface area, superior electronic conductivity and excellent stability significantly improve the activity and stability of Pd nanocatalysts [18]. Recently, graphene, as a new promising candidate among various carbon materials, has attracted tremendous attention of scientists and technologists due to its remarkable properties [19]. Owing to its 2D planar structure, excellent conductivity and large theoretical specific surface area of 2630 $m^2 \cdot g^{-1}$, graphene has garnered an incredible reputation as a support material in catalysis [20].

The synthesis of composite, combining the intrinsic properties of both Pd and graphene in the form of nanocomposite, may collectively contribute to the further enhancement of the catalytic properties of hybrid nanocatalysts [21]. The dispersion of Pd NPs on the surface of graphene is usually carried out either via post immobilization (ex situ hybridization), which involves the mixing of separate solutions of graphene and presynthesized Pd NPs or by the in-situ crystallization of NPs [22,23]. The in-situ binding is carried out via simultaneous reduction of Pd salts and graphene oxide (GRO) with several reduction techniques including chemical, thermal or electrochemical reduction [24–26]. So far, majority of Pd-graphene (Pd@graphene nanocomposite) is prepared by in-situ chemical reduction of Pd salts and GRO, which usually involves potentially hazardous and toxic reagents, starting materials, solvents, and stabilizers [27,28]. Recently, atomic layer deposition technique was used for the preparation of Pd/graphene nanocomposites [29,30], which give enhanced control over particle size and dispersion, however these techniques cannot be carried out easily in all labs and will be more difficult to scale up.

Due to growing environmental concerns, the involvement of the concepts of the green chemistry, which are designed to eliminate or reduce harmful chemicals or chemical processes that are a threat to the environment have become imminent in the field of nanocatalysis [31,32]. Therefore, applying green methods for the synthesis of catalysts and using sustainable catalytic processes may tremendously enhance the energy efficiency, environmental friendliness, and several economic benefits

for the large scale industrial processes [33]. Recently, the trends of applying green reductants—such as microorganisms, plant extracts (PEs), and amino acids—in the field of nanotechnology have garnered significant popularity [34]. Particularly, the acceptance of PEs as suitable alternatives to the chemical reductants has been steadily growing in recent years, due to their easy availability and cost effectiveness [35,36]. To date, PEs have been used for the preparation of different metallic NPs and also for the reduction of GRO, however, they are rarely applied for the in-situ preparation of graphene-metallic NP-based nanocomposites [37–39]. For instance, in our previous study, Pd@graphene nanocomposites were prepared in a facile method by the simultaneous reduction of GRO and $PdCl_2$ using *Salvadora persica* L. (miswak) root extract (RE) as bioreductant [38]. The as-prepared nanocomposites demonstrated excellent catalytic activities towards the selective oxidation of alcohols.

Herein, we demonstrate the synthesis of Pd@graphene nanocomposites using *Pulicaria glutinosa* extract (PGE) as reducing agent. The reducing ability of PGE that possesses rich phenolic contents has been already tested for the efficient synthesis of various metallic NPs [40]. Apart from this, the PGE has also been applied for the effective reduction of GRO and stabilization of HRG [41]. In view of the excellent reducing properties of the PGE for nanoparticles as well as GRO, we contemplated the study of one-step preparation of nanocomposite involving metallic NPs and GRO via simultaneous reduction. In continuation of our previous study, the PGE is now being used as a green reductant for the preparation of catalytically active Pd@graphene nanocatalyst (Scheme 1). The PGE not only acted as a reducing agent but also functioned as an in-situ functionalizing ligand to facilitate the dispersion of Pd NPs onto surface of HRG nanosheets. During this study, the catalytic activity of the Pd@graphene nanocomposites towards Suzuki-Miyura coupling reactions were tested and compared with the activity of previously prepared Pd NPs with the same PGE. Although, in both cases comparable catalytic activity is obtained, however, in the latter scenario a higher amount of Pd nanocatalyst was required to obtained similar catalytic activity. Furthermore, detailed kinetic study of catalytic coupling reactions and reusability of the catalyst was also performed. Pd@graphene nanocomposites and the products of the catalytic reactions were characterized using various microscopic and analytical techniques including gas chromatography (GC), XRD, FT-IR, UV-Vis, and HRTEM.

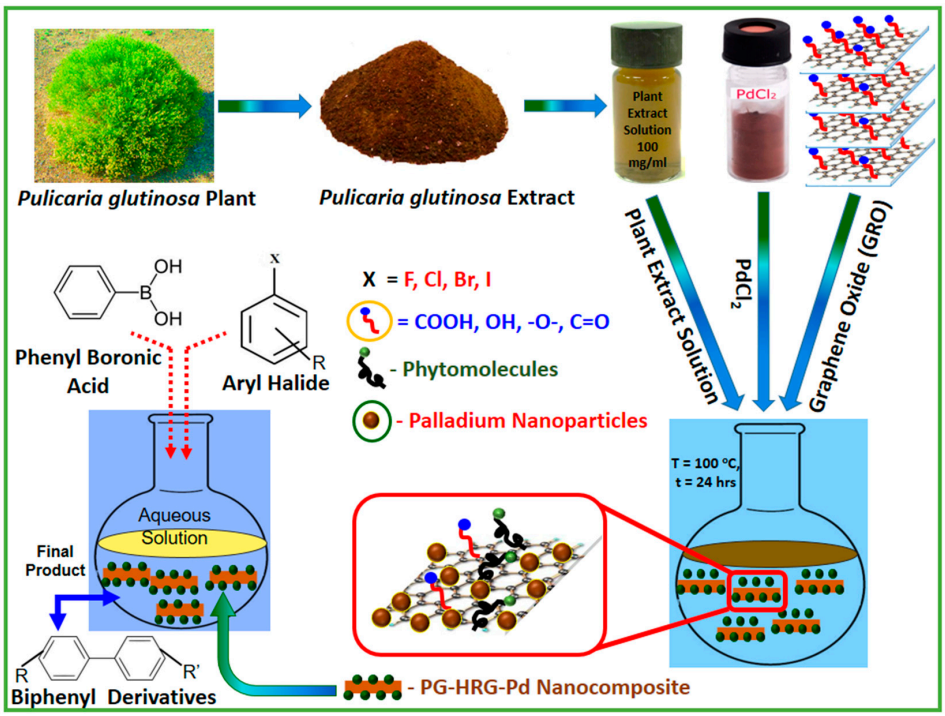

Scheme 1. Schematic illustration of the green synthesis of Pd@graphene nanocatalyst (PG-HRG-Pd) using an aqueous extract of the *P. glutinosa* and their catalytic activity for the Suzuki Miyaura coupling.

2. Results and Discussion

The preparation of Pd@graphene nanocatalyst is performed in a single step via concurrent reduction of GRO and $PdCl_2$ under mild conditions using *P. glutinosa* extract (PGE) as both reducing and stabilizing agent. To begin with, PGE was added in the required amount to the aqueous mixture of GRO and $PdCl_2$. The resulting mixture was stirred under reflux conditions until a clear color change from dark brown to black was observed, which indicated the formation of Pd@graphene nanocatalyst (PG-HRG-Pd). Furthermore, to study the effect of the amount of Pd NPs on the catalytic activities of PG-HRG-Pd nanocatalyst, two different samples including PG-HRG-Pd-1 and PG-HRG-Pd-2 were prepared by taking 50 wt % and 75 wt % of $PdCl_2$ with that of GRO, respectively, however, to monitor the influence of precursors on the density and distribution of Pd NPs on graphene support, the amount of PGE was not changed during this process.

Most of the oxygen-containing functional groups are removed during the reduction of GRO which affects the dispersing properties of HRG severely and makes it difficult to use HRG for further processing. To counter this, various additional stabilizing agents and surfactants are usually added for the dispersion of HRG, which facilitates better dispersibility of the resulting mixture. However, the PGE which is used here as a reducing agent is already known to possess various phytomolecules such as terpenoids, flavonoids, etc., which are rich in oxygen containing functional groups. These functional groups not only facilitated the simultaneous reduction of GRO and $PdCl_2$ but also helped to stabilize PG-HRG-Pd nanocatalyst by sticking on the surface of the resulting material. The oxygen containing functional groups of various phytomolecules of residual PGE, which remained attached on the surface of the HRG nanosheets, extend into the solution to provide electrostatic repulsion that stabilizes the suspension. Among these functional groups, several carboxyl and hydroxyl groups are also present, which may act as the active sites for the adsorption of Pd ions and also facilitate nucleation and growth of Pd NPs.

2.1. TEM and EDX Analysis

The presence of residual phytomolecules on the surface of PG-HRG-Pd not only enhances the aqueous dispersibility of the resulting composite, but also facilitates the homogeneous distribution of Pd NPs on the surface of HRG nanosheets. Since the nucleation of Pd starts directly on to the bound phytomolecules, it results in highly dense coating of Pd NPs on the surface of HRG sheets as shown in transmission electron micrographs (Figure 1). Detailed size distribution analysis of Pd NPs using 50 wt % ratio of Pd precursor is difficult to comment on as the particles are mostly anisotropic. The most excited morphology among metal nanoparticles is two-dimensional (2D) nano-plates (triangle or hexagonal shape). As shown in HRTEM images, the lower concentration of Pd precursor also results mostly in triangle shape Pd NPs. Here, the average edge length of Pd triangle is ~15–18 nm. The *fcc* structure of the Pd phase is confirmed by measuring the lattice *d*-spacing on top of one of the triangle shape HRTEM image which is 2.4 Å corresponding to (111) plane. However, upon using a higher concentration of Pd precursor, the morphology became isotropic with particle sizes of ~7–8 nm but it further improved the density and distribution of Pd nanoparticles onto graphene. It has provided an efficient support for the homogenous distribution of Pd NPs. In the former case where less concentration of Pd precursor is used, it could be the result of fast depletion of precursor to give rise to Ostwald ripening, resulting in bigger and anisotropic particles. This is also evidenced by very small particles in the background of bigger particles attached to support material (HRG). Whereas, in the latter case where more precursor salt is used, there is enough precursor to grow the nuclei beyond a critical radius. However, it is worth mentioning that these nanoparticles are polycrystalline with domains exposed on the surface having d-spacing (2.23 Å) corresponding to the (111) plane and also d-spacing 1.89 Å related to (200) of cubic Pd phase. The composition of the product is confirmed by energy-dispersive X-ray spectroscopy (EDX) analysis (Figure 2). Apart from the signal of Pd, the oxygen and carbon can also be seen in the EDX spectrum of PG-HRG-Pd-1, which can be attributed to the oxygen-containing functional groups of the residual phytomolecules.

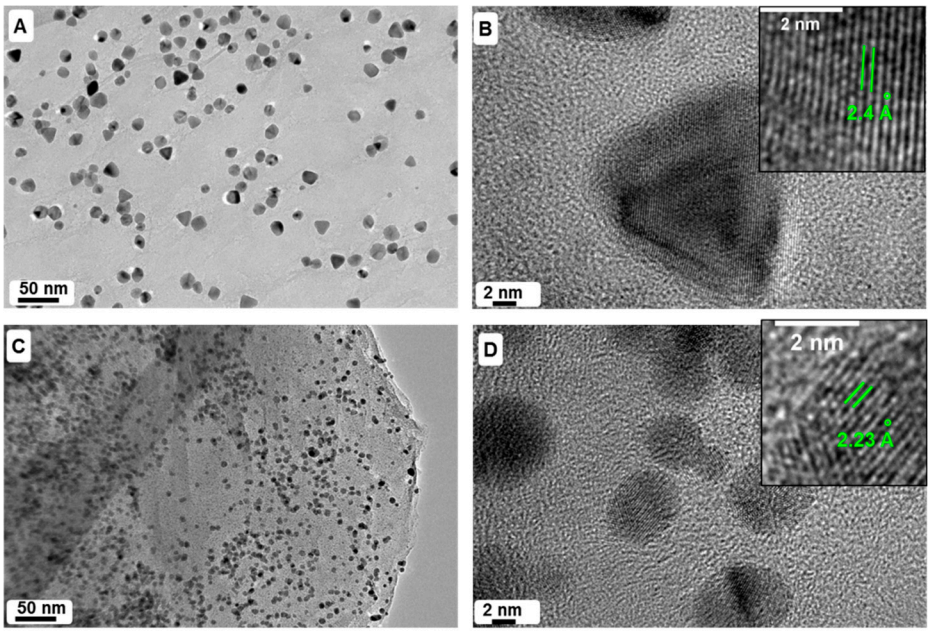

Figure 1. Transmission electron microscope (TEM) and high-resolution (HRTEM) images of the Pd@graphene nanocatalyst (PG-HRG-Pd-1) (**A**) overview PG-HRG-Pd (50 wt % ratio of Pd precursor); (**B**) HRTEM image confirming the triangular shape of Pd nanoparticles with distance between two Pd lattice fringes is 2.4 Å (inset) corresponding to (111) crystal planes of face-centered cubic (*fcc*) Pd crystals; (**C**) overview PG-HRG-Pd (75 wt % ratio of Pd precursor) showing the enhanced density of Pd nanoparticles and (**D**) high-resolution (HRTEM) image of the corresponding sample confirming the spherical morphology and also *fcc* structure of as synthesized Pd NPs (inset).

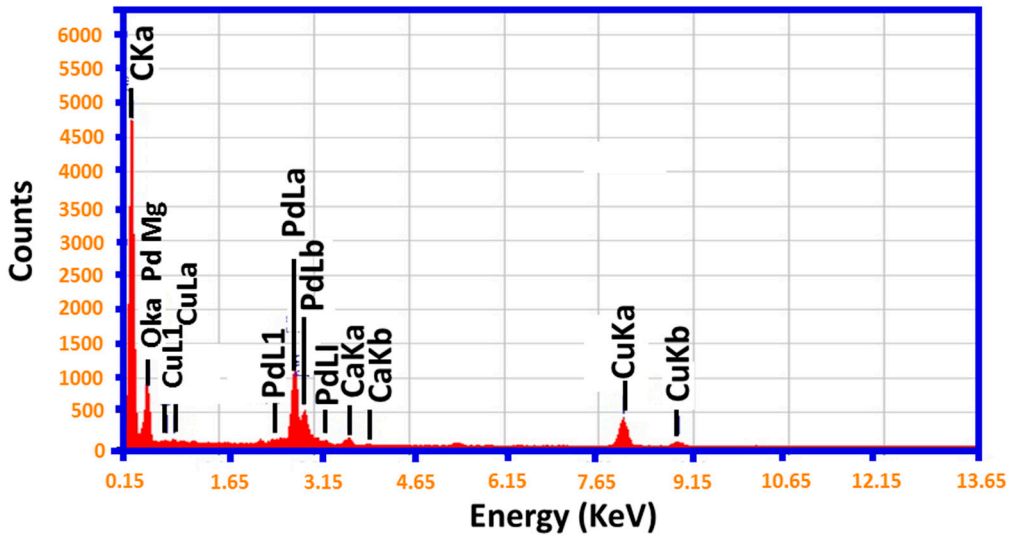

Figure 2. Energy dispersive X-ray spectrum (EDX) of as-synthesized Pd@graphene nanocatalyst (PG-HRG-Pd-1) confirming the composition of product.

2.2. Raman Spectroscopy

Raman spectroscopy was applied to monitor the reduction of GRO. Raman spectra of GRO and PG-HRG-Pd-1 nanocatalyst are displayed in Figure 3. Pristine graphene consists of two different characteristic signals, with the G and D bands situated at 1575 cm^{-1} and 1350 cm^{-1}, respectively. However, after oxidation, the sp^2 character in graphene is destroyed and various defects are formed in GRO, due to which the characteristic bands of graphene in this case are shifted to 1602 and 1340 cm^{-1},

respectively. Notably, these bands are relocated closer to their ideal positions after the reduction with PGE in the Raman spectrum of PG-HRG-Pd-1, i.e., the G band is shifted from 1602 to 1592 cm^{-1}, whereas the D band is relocated from 1340 to 1336 cm^{-1}. The emergence of some visible changes in the Raman spectra of GRO after reduction with PGE clearly reflects the formation of PG-HRG-Pd-1.

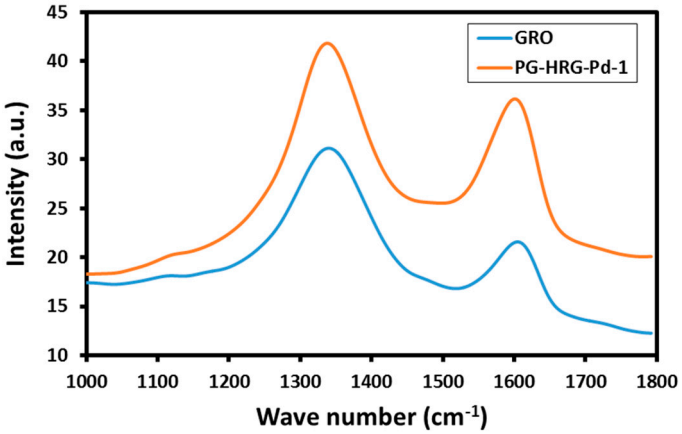

Figure 3. Raman spectra of graphene oxide (GRO) and plant extract-mediated Pd@graphene nanocatalyst (PG-HRG-Pd-1).

2.3. XRD Analysis

XRD analysis was used to confirm the phase and crystallinity of PG-HRG-Pd-1. For this purpose, XRD diffractogram of pristine graphite, GRO, and PG-HRG-Pd-1 were measured as shown in Figure 4. Typically, graphite consists of an intense reflection at 26.4° (002), which is moved to the lower brag angle in case of GRO at 10.9° corresponding to (001) plane with d-spacing of 0.81 nm, due to the addition of various oxygen containing functional groups between the graphite layers during the oxidation process [42]. Notably, in the XRD pattern after reduction, i.e., of PG-HRG-Pd-1, a broad reflection appeared at ~22.4° (002), whereas the reflection corresponding to (001) plane of GRO at 10.9° disappeared. This clearly points towards the destruction of the regular layered structure of GRO and the formation of a few layer stacked HRG sheets in PG-HRG-Pd-1 after the reduction with PGE. Besides, the XRD spectrum of PG-HRG-Pd-1 also contains several reflections at 40.02° (111), 46.49° (200), 68.05° (220), 81.74° (311), and 86.24° (222), which can be attributed to the face centered cubic (*fcc*) structure of Pd NPs on the surface of HRG (JCPDS: 87-0641, space group: Fm3m (225)).

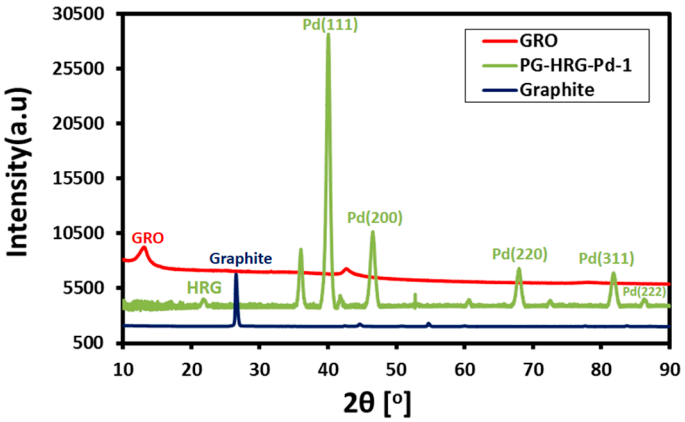

Figure 4. XRD (X-ray diffraction) diffractograms of graphite, graphene oxide (GRO), and plant extract-mediated Pd@graphene nanocatalyst (PG-HRG-Pd-1).

2.4. UV-Vis Spectral Analysis

UV spectroscopy is a very useful tool for investigating the formation of nanocatalysts and also to confirm the presence of plant extract as stabilizing agent on the surface of PG-HRG-Pd nanocatalyst. The UV spectra of $PdCl_2$, pure PGE, GRO, and PG-HRG-Pd nanocatalyst are displayed in Figure 5. Typically, GRO exhibits two absorption bands at ~230 and ~301 nm, while $PdCl_2$ possesses a distinguished absorption band at ~420 nm. The absence of these peaks in the UV spectrum of PG-HRG-Pd evidently confirms the concurrent reduction of both GRO and $PdCl_2$ and also confirms the formation of PG-HRG-Pd nanocatalyst. Notably, the UV absorption spectrum of PG-HRG-Pd exhibits two weak absorption bands at ~280 and ~325 nm which closely resemble the absorption peaks of PGE. This clearly suggests the presence of residual phytomolecules of PGE on the surface of PG-HRG-Pd nanocatalyst as stabilizing agent. This is further confirmed by FT-IR analysis by measuring the FT-IR spectra of pure PGE, GRO, and PG-HRG-Pd nanocatalyst as shown in Figure 5. Typically, the FT-IR signals belonging to the GRO either disappear or their intensities are significantly reduced after the reduction process, which in turn confirms the formation of HRG. For instance, in the FT-IR spectrum of PG-HRG-Pd the peaks at ~1630 cm^{-1} (for C=C stretching), ~1740 cm^{-1} (for C=O stretching) corresponding to the GRO disappear, whereas the intensities of some of the distinguished peaks are relatively decreased, such as a broad band at around 3440 cm^{-1} for hydroxyl groups, which points towards the reduction of GRO to HRG in PG-HRG-Pd. Upon further analysis, it was revealed that the IR spectrum of PG-HRG-Pd also bear close resemblance to the FT-IR spectrum of pure PGE. The FT-IR spectrum of the PGE exhibits signals at 3746 and 3410 cm^{-1} belonging to the OH group and a C−H peak at 2943 cm^{-1}. Apart from this, the peaks around 1753, 1622, and 1407 cm^{-1} are the typical aromatic peaks for the C−H, C−C, and C−O stretching, respectively. Whereas, the peaks corresponding to the C−O stretching of carboxylic acids, alcohols, ether, and ester groups appeared at 1264 and 1077 cm^{-1}. Expectedly, most of these peaks of PGE are also found in the FT-IR spectrum of PG-HRG-Pd, either on the same position or with slight shifts. This clearly suggests that PGE not only acted as a reducing agent but also functioned as a stabilizing agent by attaching to the surface of HRG sheets.

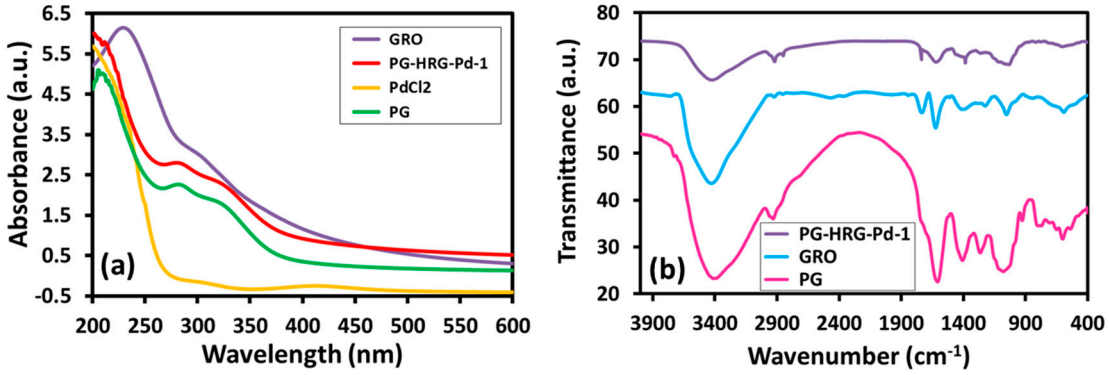

Figure 5. (**a**) UV-Vis absorption spectra of graphene oxide (GRO), Pd@graphene nanocatalyst (PG-HRG-Pd-1), palladium chloride ($PdCl_2$), and PGE; (**b**) FT-IR spectra of graphene oxide (GRO), Pd@graphene nanocatalyst (PG-HRG-Pd-1) and the PGE.

2.5. Suzuki Reaction Catalyzed by Pd@graphene Nanocatalyst

Suzuki coupling is one of the most useful methods for the synthesis of biaryls and alkene derivatives [43]. These reactions are usually carried out by using various Pd-based catalysts in different organic solvents [44]. Typically, such types of carbon–carbon couplings, including Suzuki reactions, are performed in a mixture of an organic solvent and an aqueous inorganic base, under inert conditions [45,46]. However, the concerns of the environmental impact of various chemical products and the chemical processes by which they are produced have been mounting rapidly in recent years due

to global warming. Since, majority of the chemical wastes from a reaction mixture corresponds to the solvents. Therefore, the use of water as a reaction medium, which is considered a benign solvent due to its natural abundance and physiological compatibility, may potentially contribute towards the serious efforts of reducing the environmental impacts of the organic reactions [47]. In this study, the catalytic activity of the as-synthesized PG-HRG-Pd-1 nanocatalyst was evaluated in the Suzuki Miyaura coupling of bromobenzene with phenylboronic acid in water. For this purpose, the Pd@graphene nanocomposite (PG-HRG-Pd) obtained by the simultaneous reduction of both $PdCl_2$ and GRO using PGE as reducing agent was used as a catalyst. The as-prepared nanocatalyst effectively catalyzed the reaction of various aryl halides, including, chloro, bromo, iodobenzene, chloro-benzophenone, and bromo-acetophenone with benzeneboronic acid in water containing sodium lauryl sulfate and K_3PO_4 under aerobic conditions to obtain biaryls (cf. Figure 6). The variation in the substrate structure was carried out in order to understand the catalytic performance of the nanocatalyst in the presence of different ring substituents.

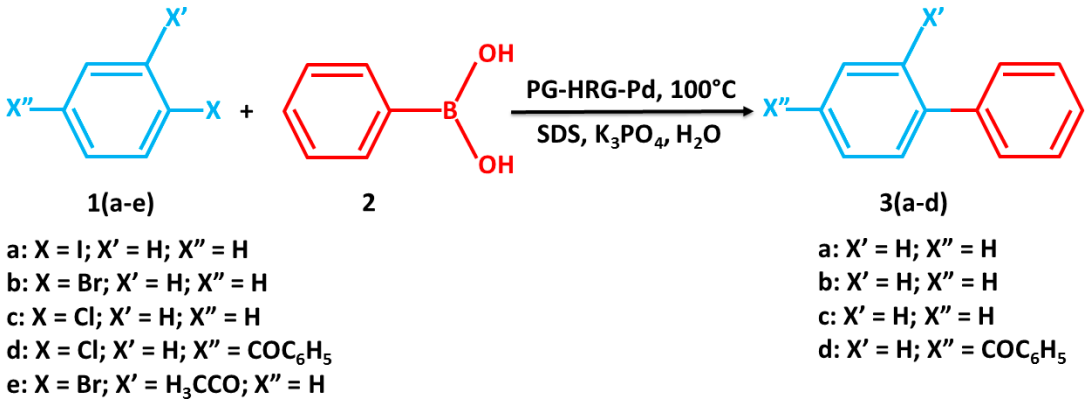

Figure 6. Schematic representation of the Suzuki reaction of iodobenzene, bromobenzene, and chlorobenzene, with phenylboronic acid under aqueous conditions.

The comparison between the catalytic performance of the two nanocatalysts, i.e., PG-HRG-Pd-1 and PG-HRG-Pd-2, has been found to be negligible whereas the catalytic performance varied extensively in the presence of different substituents. The results reveal that iodo substituted aryl halide yields the coupled product at the fastest reaction rate within 30 min for both the catalysts, however for the bromo- and chloro-substituted substrates yield ~90% and ~54% products. The 4-Chlorobenzophenone yielded least conversion product of 38%, while the 2′-Bromoacetophenone did not yielded any coupling product. This could be due to the increasing anionic nature among halogens down the group, which induces the difference in the rate of the reaction, while in the case of 2′-Bromoacetophenone, the steric hindrance from the acetate group could be responsible for not yielding any coupling product. The kinetics of the reaction were carried out using the gas chromatography (GC), which was studied by collecting the reaction mixture at equal intervals of time and quenched immediately. The graphical representation of the data is presented in the Figure 7.

The reusability of the nanocatalyst was also studied in order to find out if there is depreciation in the catalytic performance with consecutive reuse. When the catalyst was reused under similar reaction conditions, it was observed that there was a slight decrease in the percentage product formation upon consecutive reuse, which is very much unlike the results obtained when the same studies were carried out using Pd NPs prepared without graphene support [48]. Comparisons of the results obtained from reusability studies of the catalysts Pd NPs and PG-HRG-Pd-1, revealed that the depreciation of catalytic performance found by employing the PG-HRG-Pd-1, is much lower than Pd NPs wherein the catalyst loses about catalytic performance yielding an ~50% conversion product after three consecutive re-use, while PG-HRG-Pd-1 yields an ~77% conversion product after five consecutive re-uses. The graphical representation of the results obtained after several reuses of catalyst is given in Figure 8. A leaching

study was carried out in order to ascertain the leaching of Pd NPs during the catalytic process; the product was subjected to ICP-MS studies. It was found that there is 0% percent Pd NPs in the reaction mixture. This indicates that the Pd NPs formed are well supported on the HRG, hence there is no leaching of Pd NPs, which in turn results in the excellent reusability of the prepared catalyst.

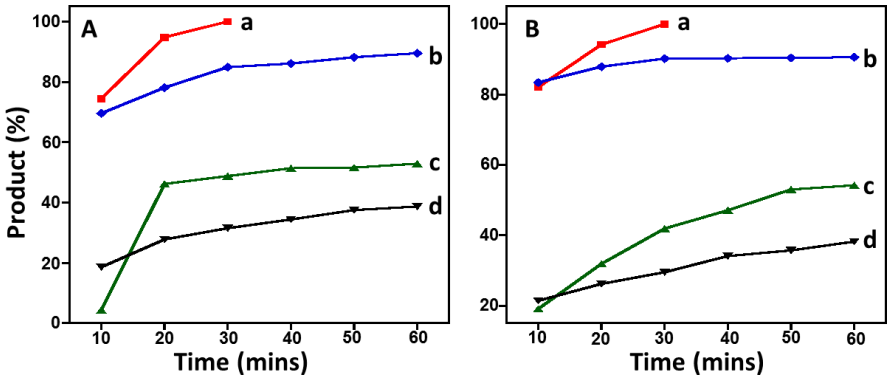

Figure 7. Time dependent conversion efficiency of the Suzuki reaction employing (**A**) PG-HRG-Pd-1 and (**B**) PG-HRG-Pd-2 for various substrates (a) iodobenzene, (b) bromobenzene, (c) chlorobenzene, and (d) chloro benzophenone with phenylboronic acid under aqueous and aerobic conditions determined by GC analysis.

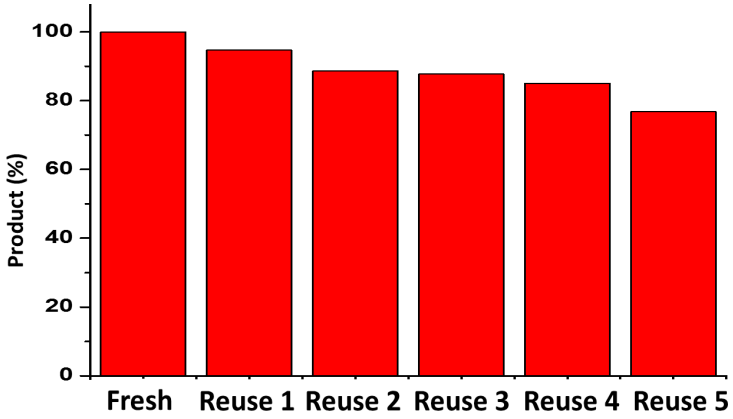

Figure 8. Graphical representation of conversion product obtained by the reuse of catalyst for the catalytic conversion of iodobenzene.

The results obtained in the present study were compared with our previously reported study [48], where in the catalyst was prepared employing the same green reducing agent without the presence of highly reduced graphene. It was observed that the prepared nanocatalyst containing graphene uses 2.5 mol % Pd NPs which is half the amount used for the previously reported, i.e., 5 mol %. However, to better understand the results obtained from both the studies, the turn over number (TON) values for both the catalysts are calculated. Upon comparison, it was observed that the TON value obtained for Pd NPs was found to be 20, while it was found to be ~74 and ~52 for the catalysts PG-HRG-Pd-1 and PG-HRG-Pd-2, respectively. A graphical representation of the comparative TON values is given in Figure 9.

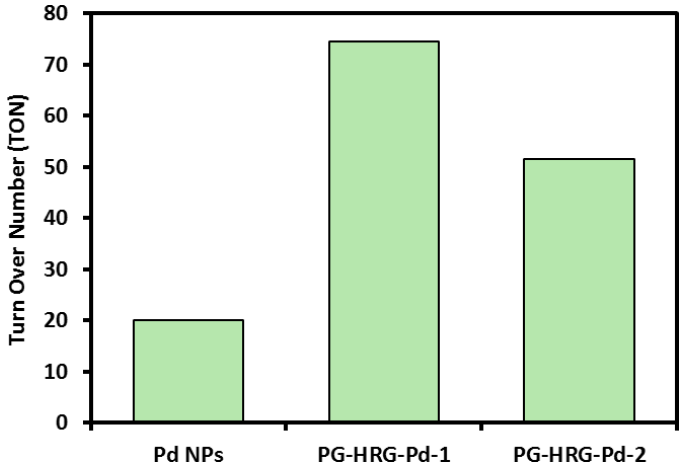

Figure 9. Graphical illustration of comparative turn over number (TON) values.

3. Materials and Methods

3.1. Materials

Natural graphite powder (99.999%, 200 mesh) was purchased from Alfa Aesar (Tewksbury, MA, USA); Palladium (II) Chloride ($PdCl_2$ 99.99%), $NaBH_4$ (96%), concentrated sulfuric acid (H_2SO_4 98%), potassium permanganate ($KMnO_4$ 99%), sodium nitrate ($NaNO_3$, 99%), hydrogen peroxide (H_2O_2, 30 wt %), bromobenzene (99.5%), sodium dodecyl sulfate (98%), phenyl boronic acid (95%), tripotassium phosphate (98%), and all organic solvents were obtained from Aldrich Chemicals (St. Louis, MI, USA) and were used directly without further purification. The details about the procedure of the collection of *P. glutinosa* and the preparation of extract are given in our previous study [40].

3.2. Methods

3.2.1. Preparation of Pd@graphene Nanocomposite (PG-HRG-Pd-1)

Graphite oxide (GO) used for the preparation of PG-HRG-Pd-1 was synthesized according to our previously reported method [41]. Initially, as-prepared graphite oxide or GO (200 mg) was dispersed in 40 mL of distilled water (DW) water and sonicated for 30 min to obtain graphene oxide (GRO) sheets. The resulting suspension was taken in a round bottom flask, to which 100 mg (0.563 mmol) of $PdCl_2$ was added. The flask was mounted with a cooling condenser, which was heated to 100 °C. Subsequently, 10 mL of an aqueous solution of the PGE (0.1 g·mL^{-1}) was added to the suspension, which was then allowed to stir for 24 h at 98 °C. Afterwards, the resulting black powder of (PG-HRG-Pd-1) was collected by filtration, and further washed with DI water several times to remove excess PGE residue and redistributed into water for sonication. This suspension was centrifuged at 4000 rpm for another 30 min. The final product was collected by vacuum filtration and dried in vacuum.

3.2.2. Suzuki Reaction Catalyzed by Pd@graphene Nanocatalyst

In a typical experiment, a mixture of sodium dodecyl sulfate (144 mg, 0.5 mmol), tripotassium phosphate (K_3PO_4, 399 mg), phenylboronic acid (146 mg, 1.2 mmol) and deionized water (20 mL) was taken in a 100 mL round bottom flask. Halobenzene (1.0 mmol) was added to this mixture under stirring, followed by the as-prepared PG-HRG-Pd-1 nanocatalyst (5 mol %, 5.32 mg). The mixture was stirred at 100 °C in an oil bath for 5 min and then extracted with ethyl acetate (3 × 20 mL). The combined organic extract was dried over anhydrous sodium sulfate (Na_2SO_4), and the resulting mixture was analyzed by gas chromatography (GC). In order to identify the product obtained from

the catalytic reaction, the as-obtained mixture was crystallized from ethanol. The coupling product obtained from using bromobenzene as starting material was isolated using column chromatography which was found to be a white powder, identified as biphenyl using ^{1}H and ^{13}C solution nuclear magnetic resonance spectroscopy (NMR) and mass spectroscopy. ^{1}H-NMR δ 8.25 (d, J = 8.3 Hz, 4H, C–CH, next to ipso), 7.25–7.26 (m, 6H, remaining protons of phenyl ring); ^{13}C-NMR δ 141.3 (2C, C–C, ipso), 128.8 (4C, CH–CH), 127.3 (2C, CH–CH, edge carbons), 127.2 (4C, C–CH, next to ipso); electron impact-mass spectrometry(EIMS) m/z 154 (M^{+}). The progress of reaction employing other substrates was monitored using gas chromatography (GC), however the coupling product was not isolated. NMR spectra's obtained are provided as Supplementary information as Figures S1 and S2.

3.3. Characterization of Catalysts

3.3.1. Transmission Electron Microscopy (TEM)

Transmission electron microscopy (TEM) and high-resolution transmission electron microscopy (HRTEM) images were obtained using a JEOL JEM 1101 (USA) instrument. The samples for the TEM measurements were prepared by suspending the composites in ethanol and were drop-cast onto a carbon-coated 200-mesh copper grid and subsequently dried at room temperature.

3.3.2. X-ray Powder Diffraction (XRD)

X-ray powder diffraction (XRD) measurements were performed on an Altima IV (Rigaku, Tokyo, Japan) instrument, which is equipped with a Cu Ka radiation source.

3.3.3. UV-Vis Spectroscopy

UV-Vis measurements were conducted on a Perkin Elmer lambda 35 (USA) UV-vis spectrophotometer (Perkin Elmer, Waltham, MA, USA). The analysis was performed in quartz cuvettes using DI water as a reference solvent. Stock solutions of PG-HRG-Pd-1 and GRO for the UV measurements were prepared by dispersing 5 mg of sample in 10 mL of DI water and sonicating for 30 min. The UV samples of GRO and PG-HRG-Pd-1 were prepared by diluting 1 mL of stock solution with 9 mL of water.

3.3.4. Fourier Transform Infrared Spectrometer (FT-IR)

Fourier transform infrared spectrometer (FT-IR) spectra were measured on a Perkin-Elmer 1000 (Perkin Elmer, Waltham, MA, USA) Fourier transform infrared spectrometer.

4. Conclusions

In summary, we have developed a green and facile method for the preparation of Pd@graphene nanocomposites and investigated their catalytic application towards the Suzuki-Miyura coupling reactions. This graphene-based novel catalyst was prepared in a single step by the spontaneous reduction of both GRO and $PdCl_2$ using *P. glutinosa* extract as reducing agent. The resultant nanocatalyst showed homogeneous distribution of Pd NPs on the surface of HRG with excellent dispersion properties, due to the presence of residual phytomolecules as stabilizing ligands. The enhanced dispersibility has enabled PG-HRG-Pd nanocatalysts to be utilized as effective catalysts for various Suzuki-Miyura coupling reactions in aqueous solution. These features, together with the ease and greenness of the synthetic process may promote the suitability of the method for large-scale production of efficient catalysts for various important organic transformations including the Suzuki-Miyura couplings. HRG support plays an excellent role due to which there is no leaching of the catalyst during the reaction, which in turn results in excellent reusability of the catalyst. Comparative studies of the TON values revealed that the prepared catalyst PG-HRG-Pd-1 is the better-performing catalyst when compared to Pd NPs prepared employing the same procedure.

Supplementary Materials: The following are available online at www.mdpi.com/2073-4344/7/1/20/s1, Figure S1: ^{1}H-NMR spectra of the Suzuki–Miyaura Coupling product. Figure S2: ^{13}C-NMR spectra of the Suzuki–Miyaura Coupling product.

Acknowledgments: This project was supported by King Saud University, Deanship of Scientific Research, College of Science, Research Centre.

Author Contributions: Muj.K., S.F.A., and Me.K. designed the project. Muj.K., S.F.A., Me.K., and M.R.S. helped to draft the manuscript. Me.K. and H.Z.A. carried out the preparation of plant extract and characterization of plant extract material. Muf.K. and M.R.S. carried out the experimental part and some part of characterization. A.A.-W., W.T., M.N.T., and M.R.H.S provided scientific guidance for successful completion of the project and also helped to draft the manuscript. All authors read and approved the final manuscript.

Conflicts of Interest: The authors declare that they have no conflict of interests.

References

1. Trost, B.M. Atom economy—A challenge for organic synthesis: Homogeneous catalysis leads the way. *Angew. Chem. Int. Ed. Engl.* **1995**, *34*, 259–281. [CrossRef]
2. Czaja, A.U.; Trukhan, N.; Müller, U. Industrial applications of metal–organic frameworks. *Chem. Soc. Rev.* **2009**, *38*, 1284–1293. [CrossRef] [PubMed]
3. Alemán, J.; Cabrera, S. Applications of asymmetric organocatalysis in medicinal chemistry. *Chem. Soc. Rev.* **2013**, *42*, 774–793. [CrossRef] [PubMed]
4. Chng, L.L.; Erathodiyil, N.; Ying, J.Y. Nanostructured catalysts for organic transformations. *Acc. Chem. Res.* **2013**, *46*, 1825–1837. [CrossRef] [PubMed]
5. Maki-Arvela, P.I.; Simakova, I.L.; Salmi, T.; Murzin, D.Y. Production of lactic acid/lactates from biomass and their catalytic transformations to commodities. *Chem. Rev.* **2013**, *114*, 1909–1971. [CrossRef] [PubMed]
6. Chu, C.K.; Liang, Y.; Fu, G.C. Silicon–carbon bond formation via nickel-catalyzed cross-coupling of silicon nucleophiles with unactivated secondary and tertiary alkyl electrophiles. *J. Am. Chem. Soc.* **2016**, *138*, 6404–6407. [CrossRef] [PubMed]
7. Ruiz-Castillo, P.; Buchwald, S.L. Applications of palladium-catalyzed C–N cross-coupling reactions. *Chem. Rev.* **2016**, *116*, 12564–12649. [CrossRef] [PubMed]
8. Han, F.-S. Transition-metal-catalyzed Suzuki-Miyaura Cross-Coupling reactions: A remarkable advance from palladium to nickel catalysts. *Chem. Soc. Rev.* **2013**, *42*, 5270–5298. [CrossRef] [PubMed]
9. Miyaura, N.; Suzuki, A. Palladium-catalyzed cross-coupling reactions of organoboron compounds. *Chem. Rev.* **1995**, *95*, 2457–2483. [CrossRef]
10. Deraedt, C.; Astruc, D. "Homeopathic" palladium nanoparticle catalysis of cross carbon–carbon coupling reactions. *Acc. Chem. Res.* **2013**, *47*, 494–503. [CrossRef] [PubMed]
11. Hattori, T.; Tsubone, A.; Sawama, Y.; Monguchi, Y.; Sajiki, H. Palladium on carbon-catalyzed Suzuki-Miyaura coupling reaction using an efficient and continuous flow system. *Catalysts* **2015**, *5*, 18–25. [CrossRef]
12. Gniewek, A.; Ziółkowski, J.J.; Trzeciak, A.M.; Zawadzki, M.; Grabowska, H.; Wrzyszcz, J. Palladium nanoparticles supported on alumina-based oxides as heterogeneous catalysts of the Suzuki-Miyaura reaction. *J. Catal.* **2008**, *254*, 121–130. [CrossRef]
13. Kalidindi, S.B.; Jagirdar, B.R. Nanocatalysis and prospects of green chemistry. *ChemSusChem* **2012**, *5*, 65–75. [CrossRef] [PubMed]
14. Manabe, K. Palladium catalysts for cross-coupling reaction. *Catalysts* **2015**, *5*, 38–39. [CrossRef]
15. Wang, J.; Gu, H. Novel metal nanomaterials and their catalytic applications. *Molecules* **2015**, *20*, 17070–17092. [CrossRef] [PubMed]
16. Ohtaka, A.; Okagaki, T.; Hamasaka, G.; Uozumi, Y.; Shinagawa, T.; Shimomura, O.; Nomura, R. Application of "boomerang" linear polystyrene-stabilized Pd nanoparticles to a series of C–C coupling reactions in water. *Catalysts* **2015**, *5*, 106–118. [CrossRef]
17. Gautam, P.; Dhiman, M.; Polshettiwar, V.; Bhanage, B.M. KCC-1 supported palladium nanoparticles as an efficient and sustainable nanocatalyst for carbonylative Suzuki-Miyaura Cross-Coupling. *Green Chem.* **2016**, *18*, 5890–5899. [CrossRef]
18. Adib, M.; Karimi-Nami, R.; Veisi, H. Palladium NPs supported on novel imino-pyridine-functionalized MWCNTs: Efficient and highly reusable catalysts for the Suzuki-Miyaura and Sonogashira coupling reactions. *New J. Chem.* **2016**, *40*, 4945–4951. [CrossRef]

19. Raccichini, R.; Varzi, A.; Passerini, S.; Scrosati, B. The role of graphene for electrochemical energy storage. *Nat. Mater.* **2015**, *14*, 271–279. [CrossRef] [PubMed]
20. Fan, X.; Zhang, G.; Zhang, F. Multiple roles of graphene in heterogeneous catalysis. *Chem. Soc. Rev.* **2015**, *44*, 3023–3035. [CrossRef] [PubMed]
21. Khan, M.; Tahir, M.N.; Adil, S.F.; Khan, H.U.; Siddiqui, M.R.H.; Al-warthan, A.A.; Tremel, W. Graphene based metal and metal oxide nanocomposites: Synthesis, properties and their applications. *J. Mater. Chem. A* **2015**, *3*, 18753–18808. [CrossRef]
22. Metin, Ö.; Kayhan, E.; Özkar, S.; Schneider, J.J. Palladium nanoparticles supported on chemically derived graphene: An efficient and reusable catalyst for the dehydrogenation of ammonia borane. *Int. J. Hydrogen Energy* **2012**, *37*, 8161–8169. [CrossRef]
23. Xu, W.; Wang, X.; Zhou, Q.; Meng, B.; Zhao, J.; Qiu, J.; Gogotsi, Y. Low-temperature plasma-assisted preparation of graphene supported palladium nanoparticles with high hydrodesulfurization activity. *J. Mater. Chem.* **2012**, *22*, 14363–14368. [CrossRef]
24. Zhang, Y.; Shu, H.; Chang, G.; Ji, K.; Oyama, M.; Liu, X.; He, Y. Facile synthesis of palladium–graphene nanocomposites and their catalysis for electro-oxidation of methanol and ethanol. *Electrochim. Acta* **2013**, *109*, 570–576. [CrossRef]
25. Liu, Y.; Liu, L.; Shan, J.; Zhang, J. Electrodeposition of palladium and reduced graphene oxide nanocomposites on foam-nickel electrode for electrocatalytic hydrodechlorination of 4-chlorophenol. *J. Hazard. Mater.* **2015**, *290*, 1–8. [CrossRef] [PubMed]
26. Konda, S.K.; Chen, A. One-step synthesis of Pd and reduced graphene oxide nanocomposites for enhanced hydrogen sorption and storage. *Electrochem. Commun.* **2015**, *60*, 148–152. [CrossRef]
27. Li, Y.; Fan, X.; Qi, J.; Ji, J.; Wang, S.; Zhang, G.; Zhang, F. Palladium nanoparticle-graphene hybrids as active catalysts for the Suzuki reaction. *Nano Res.* **2010**, *3*, 429–437. [CrossRef]
28. Fu, L.; Lai, G.; Zhu, D.; Jia, B.; Malherbe, F.; Yu, A. Advanced catalytic and electrocatalytic performances of polydopamine-functionalized reduced graphene oxide-palladium nanocomposites. *ChemCatChem* **2016**, *8*, 2975–2980. [CrossRef]
29. Yan, H.; Cheng, H.; Yi, H.; Lin, Y.; Yao, T.; Wang, C.; Li, J.; Wei, S.; Lu, J. Single-Atom Pd_1/Graphene Catalyst Achieved by Atomic Layer Deposition: Remarkable Performance in Selective Hydrogenation of 1,3-Butadiene. *J. Am. Chem. Soc.* **2015**, *137*, 10484–10487. [CrossRef] [PubMed]
30. Van Bui, H.; Grillo, F.; Helmer, R.; Goulas, A.; van Ommen, J.R. Controlled growth of palladium nanoparticles on graphene nanoplatelets via scalable atmospheric pressure atomic layer deposition. *J. Phys. Chem. C* **2016**, *120*, 8832–8840. [CrossRef]
31. Narayanan, R. Synthesis of green nanocatalysts and industrially important green reactions. *Green Chem. Lett. Rev.* **2012**, *5*, 707–725. [CrossRef]
32. Majeed, M.I.; Lu, Q.; Yan, W.; Li, Z.; Hussain, I.; Tahir, M.N.; Tremel, W.; Tan, B. Highly water-soluble magnetic iron oxide (Fe_3O_4) nanoparticles for drug delivery: Enhanced in vitro therapeutic efficacy of doxorubicin and MION conjugates. *J. Mater. Chem. B* **2013**, *1*, 2874–2884. [CrossRef]
33. Polshettiwar, V.; Varma, R.S. Green chemistry by nano-catalysis. *Green Chem.* **2010**, *12*, 743–754. [CrossRef]
34. Adil, S.F.; Assal, M.E.; Khan, M.; Al-Warthan, A.; Siddiqui, M.R.H.; Liz-Marzán, L.M. Biogenic synthesis of metallic nanoparticles and prospects toward green chemistry. *Dalton Trans.* **2015**, *44*, 9709–9717. [CrossRef] [PubMed]
35. Alam, M.N.; Roy, N.; Mandal, D.; Begum, N.A. Green chemistry for nanochemistry: Exploring medicinal plants for the biogenic synthesis of metal NPs with fine-tuned properties. *RSC Adv.* **2013**, *3*, 11935–11956. [CrossRef]
36. Peralta-Videa, J.R.; Huang, Y.; Parsons, J.G.; Zhao, L.; Lopez-Moreno, L.; Hernandez-Viezcas, J.A.; Gardea-Torresdey, J.L. Plant-based green synthesis of metallic nanoparticles: Scientific curiosity or a realistic alternative to chemical synthesis? *Nanotechnol. Environ. Eng.* **2016**, *1*, 4. [CrossRef]
37. Kharissova, O.V.; Dias, H.R.; Kharisov, B.I.; Pérez, B.O.; Pérez, V.M.J. The greener synthesis of nanoparticles. *Trends Biotechnol.* **2013**, *31*, 240–248. [CrossRef] [PubMed]
38. Al-Marri, A.H.; Khan, M.; Shaik, M.R.; Mohri, N.; Adil, S.F.; Kuniyil, M.; Alkhathlan, H.Z.; Al-Warthan, A.; Tremel, W.; Tahir, M.N. Green synthesis of Pd@graphene nanocomposite: Catalyst for the selective oxidation of alcohols. *Arab. J. Chem.* **2016**, *9*, 835–845. [CrossRef]

39. Nasrollahzadeh, M.; Maham, M.; Rostami-Vartooni, A.; Bagherzadeh, M.; Sajadi, S.M. Barberry fruit extract assisted in situ green synthesis of Cu nanoparticles supported on a reduced graphene oxide–Fe_3O_4 nanocomposite as a magnetically separable and reusable catalyst for the *O*-arylation of phenols with aryl halides under ligand-free conditions. *RSC Adv.* **2015**, *5*, 64769–64780.
40. Khan, M.; Khan, M.; Kuniyil, M.; Adil, S.F.; Al-Warthan, A.; Alkhathlan, H.Z.; Tremel, W.; Tahir, M.N.; Siddiqui, M.R.H. Biogenic synthesis of palladium nanoparticles using *Pulicaria glutinosa* extract and their catalytic activity towards the Suzuki coupling reaction. *Dalton Trans.* **2014**, *43*, 9026–9031. [CrossRef] [PubMed]
41. Khan, M.; Al-Marri, A.H.; Khan, M.; Mohri, N.; Adil, S.F.; Al-Warthan, A.; Siddiqui, M.R.H.; Alkhathlan, H.Z.; Berger, R.; Tremel, W. *Pulicaria glutinosa* plant extract: A green and eco-friendly reducing agent for the preparation of highly reduced graphene oxide. *RSC Adv.* **2014**, *4*, 24119–24125. [CrossRef]
42. Movahed, S.K.; Dabiri, M.; Bazgir, A. Palladium nanoparticle decorated high nitrogen-doped graphene with high catalytic activity for Suzuki-Miyaura and Ullmann-type coupling reactions in aqueous media. *Appl. Catal. A Gen.* **2014**, *488*, 265–274. [CrossRef]
43. Polshettiwar, V.; Decottignies, A.; Len, C.; Fihri, A. Suzuki-Miyaura Cross-Coupling reactions in aqueous media: Green and sustainable syntheses of biaryls. *ChemSusChem* **2010**, *3*, 502–522. [CrossRef] [PubMed]
44. Dhakshinamoorthy, A.; Asiri, A.M.; Garcia, H. Metal–organic frameworks catalyzed C–C and C–heteroatom coupling reactions. *Chem. Soc. Rev.* **2015**, *44*, 1922–1947. [CrossRef] [PubMed]
45. Littke, A.F.; Dai, C.; Fu, G.C. Versatile catalysts for the Suzuki Cross-Coupling of arylboronic acids with aryl and vinyl halides and triflates under mild conditions. *J. Am. Chem. Soc.* **2000**, *122*, 4020–4028. [CrossRef]
46. Martin, R.; Stephen, L.B. Palladium-catalyzed Suzuki−Miyaura Cross-Coupling reactions employing dialkylbiaryl phosphine ligands. *Acc. Chem. Res.* **2008**, *41*, 1461–1473. [CrossRef] [PubMed]
47. Handa, S.; Wang, Y.; Gallou, F.; Lipshutz, B.H. Sustainable Fe–ppm Pd nanoparticle catalysis of Suzuki-Miyaura Cross-Couplings in water. *Science* **2015**, *349*, 1087–1091. [CrossRef] [PubMed]
48. Khan, M.; Albalawi, G.H.; Shaik, M.R.; Khan, M.; Adil, S.F.; Kuniyil, M.; Alkhathlan, H.Z.; Al-Warthan, A.; Siddiqui, M.R.H. Miswak mediated green synthesized palladium nanoparticles as effective catalysts for the Suzuki coupling reactions in aqueous media. *J. Saudi Chem. Soc.* **2016**, in press. [CrossRef]